

# Einstein Cluster as Central Spiky Distribution of Galactic Dark Matter

Kei-ichi Maeda,<sup>1,2</sup> Vitor Cardoso,<sup>3,4</sup> and Anzhong Wang<sup>5</sup>

<sup>1</sup> *Department of Physics, Waseda University,  
3-4-1 Okubo, Shinjuku, Tokyo 169-8555, Japan*

<sup>2</sup> *Center for Gravitational Physics and Quantum Information,  
Yukawa Institute for Theoretical Physics, Kyoto University, 606-8502, Kyoto, Japan*

<sup>3</sup> *CENTRA, Departamento de Física, Instituto Superior Técnico – IST,  
Universidade de Lisboa – UL, Avenida Rovisco Pais 1, 1049 Lisboa, Portugal and*

<sup>4</sup> *Niels Bohr International Academy, Niels Bohr Institute,  
Blegdamsvej 17, 2100 Copenhagen, Denmark*

<sup>5</sup> *GCAP-CASPER, Physics Department, Baylor University, Waco, Texas 76798-7316, US*  
(Dated: October 8, 2024)

Using the Einstein cluster models, we construct a fully relativistic, spherically symmetric, spiky structure of matter distribution near a supermassive black hole. We introduce and discuss three simple toy models, together with a more realistic model, which includes a Hernquist-type distribution with a typical galaxy scale. We find that the innermost stable circular orbit (ISCO) depends on the details of the environment, and lies between the photon radius (at  $3M_{\text{BH}}$ ) and the ISCO radius of an isolated black hole of mass  $M_{\text{BH}}$  (at  $6M_{\text{BH}}$ ).

PACS numbers:

## I. INTRODUCTION

The nature of dark matter (DM) and its role in standard model of particle physics is one of the most mysterious problems in modern cosmology. We know it exists via its gravitational effects, but we are ignorant of its properties, including mass or couplings to other fields. The range of possibilities is extremely large: DM could be a new fundamental particle, or it could simply be a large amount of tiny primordial black holes (PBHs), or a plethora of new fields, among other possibilities. Despite the numerous searches for specific DM candidates, no compelling candidate has yet been found [1–6].

One possible approach to understand the nature and local distribution of DM consists on studying specific events near a supermassive black hole (SMBH) or intermediate mass black hole (IMBH). The annihilation of DM particles and consequent sourcing of high luminosity events has been discussed as a possible smoking gun of DM [7]. A powerful alternative consists on the observation of gravitational waves, which is to a large extent independent of the strength of the coupling between DM and the standard model of particle physics [8–10]. In addition, precise monitoring of the periastron shift and overall motion of stars nearby BHs could also reveal some features of DM distribution [11–14].

Most DM distributions are studied in a fixed, flat-space background. One of the most popular distributions is the Navarro–Frenk–White (NFW) profile, which is consistent with observations and  $N$ -body simulations. Other profiles such as Hernquist-type distribution have also been pro-

posed [15]. The adiabatic growth of a BH may induce a spiky, dense structure near BHs [7]. The relativistic extension of the spiky structure near SMBH was given by [16]. One of the striking conclusions of these works is that the inner boundary of the spiky DM distribution is below the innermost stable circular orbit (ISCO) radius; in particular, the inner boundary is located at an areal radius  $4M_{\text{BH}}$  for a spherically symmetric system, with  $M_{\text{BH}}$  the BH mass.

The DM distribution close to BHs is particularly interesting: its density in the strong gravity regime can be considerably large, and hence effects on gravitational wave emission can be important. Thus, in the context of observations concerning events in highly dynamical, strong-field gravity, a careful modelling of DM distribution in a fully general-relativistic setting is required. Especially, when we take into account the self-gravity of the DM distribution, the curved spacetime description is no longer that of a vacuum Kerr geometry. Fully general relativistic solutions describing spherically symmetric BHs immersed in environments were discussed recently [9] assuming an Hernquist-type DM distribution. The DM is distributed all throughout the BH exterior regions in the original work, violating the dominant energy condition in a region close to the horizon. A simple modification of the original profile eliminates this issue [17]; other analytic form of DM distribution was also given in Ref. [18, 19].

In this note, we provide simple analytic models with spiky DM distribution within the so-called Einstein cluster construction. In fact, although we have DM in mind, our results apply as well for

standard, baryonic matter environments. There are several works on DM distribution by use of the Einstein cluster [20–22]. Here we focus on the possibility that some distributions may yield smaller ISCO radius, below the ISCO radius of the central BH ( $6M_{\text{BH}}$ ).

After we introduce the basic equations for the Einstein cluster in §II, we discuss on how to find the ISCO radius of the DM distribution when we take into account self-gravity of DM in §III. We then present three toy models with the ISCO radius smaller than  $6M_{\text{BH}}$  in §IV. In §V, we present a slightly realistic models with a typical galactic scale where the distribution profile changes. The summary and discussion follow in §VI.

## II. A SPHERICALLY SYMMETRIC EINSTEIN CLUSTER SPACETIME

We consider a spherically symmetric spacetime, described by the line element

$$ds^2 = -f(r)dt^2 + \frac{dr^2}{1 - \frac{2m(r)}{r}} + r^2 d\Omega^2. \quad (2.1)$$

In vacuum, the general solution is the Schwarzschild spacetime,

$$m(r) = M_{\text{BH}}, \quad f(r) = f_0 \left(1 - \frac{2M_{\text{BH}}}{r}\right),$$

where  $M_{\text{BH}}$  is the BH mass and  $f_0$  is an integration constant.

In this note, we consider DM distribution outside the event horizon. We assume that DM is composed of particles moving along circular geodesics just as the Einstein cluster. Since the radial component of the pressure is assumed to be zero ( $P_r = 0$ ) as we will show it explicitly for the present model, the Einstein equations and energy-momentum conservation give

$$m' = 4\pi r^2 \rho, \quad (2.2)$$

$$\frac{f'}{f} = \frac{2m(r)}{r(r - 2m(r))}, \quad (2.3)$$

$$P_t = \frac{m(r)}{2(r - 2m(r))} \rho. \quad (2.4)$$

For circular orbits, the 4-velocity obeys

$$u_0 = -E, \quad u^0 = \frac{E}{f},$$

$$u_\phi = L_z, \quad u^\phi = \frac{L_z}{r^2 \sin^2 \theta},$$

$$r^4 (u^\theta)^2 = L^2 - \frac{L_z^2}{\sin^2 \theta}.$$

With the normalization  $u^\mu u_\mu = -1$ , we find the radial equation

$$\frac{f(r)}{1 - \frac{2m(r)}{r}} \left(\frac{dr}{d\tau}\right)^2 = E^2 - V_{\text{eff}}^2(r; L),$$

where the effective potential  $V_{\text{eff}}^2$  is defined by

$$V_{\text{eff}}^2 = f(r) \left(1 + \frac{L^2}{r^2}\right). \quad (2.5)$$

The radius of a circular orbit is given by the equation

$$\frac{dV_{\text{eff}}^2}{dr} = \frac{2f}{r^3(r - 2m(r))} [m(r)r^2 - L^2(r - 3m(r))] = 0, \quad (2.6)$$

where we used Eq. (2.3).

The energy  $E$  and angular momentum  $\mathbf{L}$  ( $L = |\mathbf{L}|, L_z$ ) of a particle on a circular orbit in the spacetime (2.1) are given by

$$E^2 = f(r) \left(1 + \frac{L^2}{r^2}\right) = \frac{r - 2m(r)}{r - 3m(r)} f(r), \quad (2.7)$$

$$L_z = L \cos \theta, \quad (2.8)$$

$$L^2 = \frac{m(r)r^2}{r - 3m(r)}. \quad (2.9)$$

Note that since  $m(r) > 0$  and  $f > 0$ , we find that  $r > 3m(r)$  from the above equations, which means that photon sphere in the present model does not exist inside the dark DM distribution.

The energy-momentum tensor of  $N$  particles is given by

$$T^\mu_\nu = \mu_0 \sum_{I=1}^N \int d\tau_I \frac{u_I^\mu u_{I\nu}}{\sqrt{-g}} \delta(x - z_I),$$

where  $\mu_0$  is a particle mass and  $u_I^\mu$  is 4-velocity of the  $I$ -th particle in the spacetime given by the metric (2.1). The energy density and pressures are given by

$$\begin{aligned}\rho(\mathbf{r}) &= u^0 u_0 n(\mathbf{r}) = \frac{E^2}{f} n(\mathbf{r}) = \left(1 + \frac{L^2}{r^2}\right) n(\mathbf{r}) = \frac{r - 2m(r)}{r - 3m(r)} n(\mathbf{r}), \\ P_r(\mathbf{r}) &= 0, \\ P_t(\mathbf{r}) &= \langle u^\phi u_\phi \rangle n(\mathbf{r}) = \frac{L^2 \langle \cos^2 \theta \rangle}{r^2} n(\mathbf{r}) = \frac{L^2}{2r^2} n(\mathbf{r}) = \frac{m(r)}{2(r - 3m(r))} n(\mathbf{r}),\end{aligned}$$

where  $n(\mathbf{r})$  is the unknown distribution function of particles, determined by the energy density  $\rho(\mathbf{r})$ .

### III. ISCO RADIUS AND CONDITIONS NEAR ISCO RADIUS

We then look for the radius of the ISCO in the spacetime (2.1), which is obtained by Eq.(2.6) and

$$\frac{d^2 V_{\text{eff}}^2}{dr^2} = \frac{2f}{r^4(r - 2m(r))^2} \times [m' r^4 - 2mr^2(r - 2m) + L^2 (m' r^2 + 3(r - 2m)(r - 4m))] = 0, \quad (3.1)$$

where we again used Eq. (2.3). Eliminating  $L^2$ , we find the stability condition for the circular orbit

$$r^2 m'(r) + r m(r) - 6m^2(r) \geq 0, \quad (3.2)$$

where the equality corresponds to the inflection point. Hence solving the equation

$$r^2 m'(r) + r m(r) - 6m^2(r) = 0, \quad (3.3)$$

we obtain the ISCO radius  $r_I$  as the minimum value of the possible solutions. We then find the energy  $E_{\text{ISCO}}$  and angular momentum  $L_{\text{ISCO}}$  of a particle at the ISCO radius from Eqs. (2.7) and (2.9) by inserting  $r = r_I$ .

Now we consider the behaviour of metric and matter distribution near the ISCO radius. We assume there is no matter fluid below the ISCO radius  $r_I$ . We then assume mass function  $m(r)$  near the ISCO radius as

$$m(r) = M_{\text{BH}} [1 + \alpha(r - r_I)^p / M_{\text{BH}}^p] \quad (r \geq r_I),$$

where  $\alpha > 0$ . There is no solution for  $p < 0$ . In the case of  $p = 0$ , we have to put a mass shell at  $r_I$  and  $r_I = 6m(r_I) = 6(M_{\text{BH}} + \alpha)$ , which is a trivial case. When  $0 < p < 1$ ,  $m'$  diverges at  $r_I$  and there is no solution for Eq. (3.3). For  $p > 1$ , we find  $r_I = 6M_{\text{BH}}$  because  $m'(r_I) = 0$ . This gives usual BH ISCO radius. Note that if the energy density vanishes at the ISCO radius, i.e.,  $\rho \propto (r - r_I)^{\tilde{p}}$  ( $\tilde{p} > 0$ ), we find  $p = \tilde{p} + 1 > 1$ .

We find a non-trivial solution when  $p = 1$ . Eq. (3.3) becomes

$$\alpha r_I^2 + M_{\text{BH}} r_I - 6M_{\text{BH}}^2 = 0, \quad (3.4)$$

i.e.,

$$m(r) = M_{\text{BH}} + \alpha(r - r_I) \quad (r \geq r_I), \quad (3.5)$$

$$r_I = \frac{M_{\text{BH}}}{2\alpha} (-1 + \sqrt{1 + 24\alpha}). \quad (3.6)$$

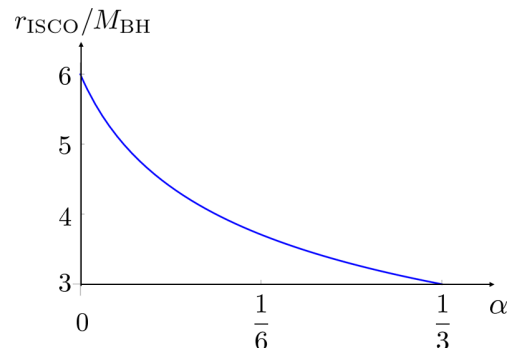


FIG. 1: The relation between the ISCO radius ( $r_I$ ) and the parameter  $\alpha$  for the case of  $p = 1$ .

The condition of  $r > 3m(r)$  gives  $\alpha < \frac{1}{3}$ . We show  $r_I$  in terms of  $\alpha$  in Fig. 1. In the limit of  $\alpha \rightarrow \frac{1}{3}$ , we find  $r_I \rightarrow 3M_{\text{BH}}$ , while for  $\alpha = 0$ , we recover the vacuum BH ISCO radius ( $r_I \rightarrow 6M_{\text{BH}}$ ).

### IV. SIMPLE TOY MODELS

One interesting question is whether DM can exist inside the vacuum BH ISCO radius ( $< 6M_{\text{BH}}$ ). In a realistic DM distribution, we have to take into account the initial conditions and diffusion process of particles in a realistic situation. However, in this note, we focus solely on the above point concern-

ing existence, and construct simple models with  $r_I < 6M_{\text{BH}}$ , giving mass distribution  $m(r)$ .

In what follows, we shall normalize all quantities by the BH mass and set  $M_{\text{BH}} = 1$ .

### A. Model I (“Isothermal” distribution)

First we assume the (simplistic) mass function

$$m(r) = 1 + \alpha(r - r_I),$$

where  $0 < \alpha < 1/3$  is a constant. We find

$$\rho = \frac{m'}{4\pi r^2} = \frac{\alpha}{4\pi r^2},$$

an “isothermal”-like distribution. The metric function  $f$  is easily integrated,

$$f = \frac{c_0}{r} (r - r_*)^{\frac{1}{1-2\alpha}} \quad (r \geq r_I), \quad (4.1)$$

where

$$r_* \equiv \frac{2(1 - \alpha r_I)}{1 - 2\alpha},$$

and  $c_0$  is an integration constant, fixed by the outer boundary conditions. Stability condition (3.2) is always satisfied. Interestingly, for  $\alpha = 1/3$  and ISCO radius at  $r_I = 3$  (the photon sphere radius), then every point satisfies the inflection condition (3.3). Every point is marginally stable.

Since  $m(r) \rightarrow \infty$  as  $r \rightarrow \infty$ , we assume that matter distribution is truncated, and exists only between  $r_I$  and  $r_O$ . The total mass of the system is given by  $M = m(r_O) = 1 + \alpha(r_O - r_I)$ . Outside, the metric is given by the Schwarzschild metric with mass  $M$ . We can confirm that the outer radius  $r_O$  is always larger than the ISCO radius of the mass  $M$ , i.e.,  $r_O \geq 6M$ . The metric is given by

$$m(r) = \begin{cases} 1 & (r < r_I) \\ 1 + \alpha(r - r_I) & (r_I < r < r_O) \\ M & (r > r_O) \end{cases},$$

$$f(r) = \begin{cases} f_0 \left(1 - \frac{2}{r}\right) & (r < r_I) \\ \frac{c_0}{r} (r - r_*)^{\frac{1}{1-2\alpha}} & (r_I < r < r_O) \\ 1 - \frac{2M}{r} & (r > r_O) \end{cases},$$

where

$$f_0 = \frac{r_O - 2M}{r_I - 2} \left( \frac{r_I - r_*}{r_O - r_*} \right)^{\frac{1}{1-2\alpha}},$$

$$c_0 = \frac{r_O - 2M}{(r_O - r_*)^{\frac{1}{1-2\alpha}}}.$$

Note that the tangential pressure is given by

$$P_t = \frac{m(r)\rho(r)}{2(r - 2m(r))}.$$

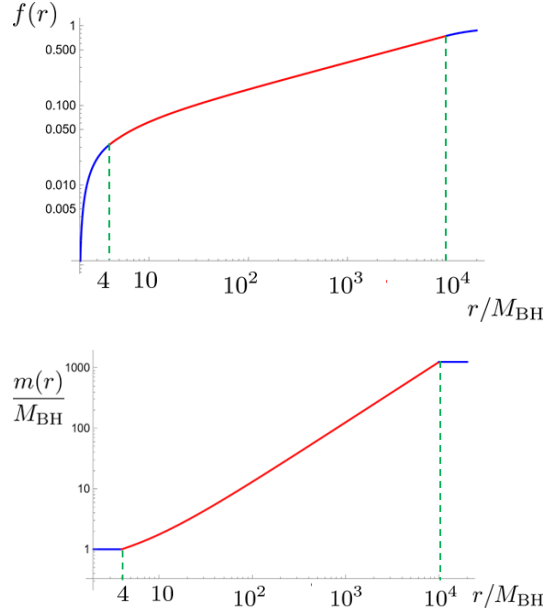


FIG. 2: Metric functions for Model I,  $f(r)$  (top) and  $m(r)$  (bottom). We set  $r_I = 4M_{\text{BH}}$  ( $\alpha = \frac{1}{8}$ ) and  $r_O = 10^4 M_{\text{BH}}$ , which gives  $M = 1250.5M_{\text{BH}}$ .

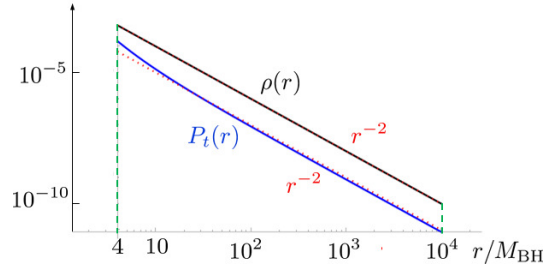


FIG. 3: The distributions of the energy density  $\rho$  and tangential pressure  $P_t$  for Model I. The parameters are the same as those in Fig. 2.

The metric functions  $f(r)$  and  $m(r)$  of the present model are shown in Fig. 2, and the energy density  $\rho$  and tangential pressure  $P_t$  in Fig. 3. We set  $\alpha = 1/8$ , which gives  $r_I = 4M_{\text{BH}}$ . We choose  $r_O = 10^4 M_{\text{BH}}$ . These parameters give  $M = 1250.5M_{\text{BH}}$ ,  $r_* = \frac{4}{3}M_{\text{BH}}$ ,  $f_0 \approx 0.0644$  and  $c_0 \approx 0.0348$ .

### B. Model II

The distribution above, with a very specific choice of ISCO radius, allows for marginally stable timelike circular geodesics in the entire space-time. We also find a curious, analytic model that doesn’t fine tune the integration constants, and for

which every point in the matter distribution is an inflection point. We have to solve Eq. (3.3) for  $r_1 \leq r \leq r_O$ . Imposing  $r > 3m(r)$ , we obtain

$$m(r) = \frac{r}{3[1 + (r/r_c)^2]}, \quad (4.2)$$

where  $r_c$  is an integration constant. The density distribution is

$$\rho = \frac{m'}{4\pi r^2} = \frac{1 - (r/r_c)^2}{12\pi r^2 [1 + (r/r_c)^2]^2}.$$

The density vanishes at  $r = r_c$ , thus the outer radius of the distribution must be  $r_O \leq r_c$ . From the stability condition, i.e., the outer radius is larger than the ISCO radius of the total mass  $M_O$  ( $r_O \geq 6M_O = 6m(r_O)$ ), we find

$$r_O \geq \frac{2r_O}{[1 + (r_O/r_c)^2]},$$

which gives  $r_O \geq r_c$ . As a result, the outer radius must be  $r_O = r_c$ .

For the metric function  $f$ , we obtain

$$f = \frac{c_0 r^2}{1 + 3(r/r_O)^2},$$

with  $c_0$  an integration constant.

Since the outside ( $r > r_O$ ) and inside ( $r < r_1$ ) of the Einstein cluster are assumed to be in vacuum, the continuity conditions at  $r_1$  and  $r_O$  yield,

$$m = \begin{cases} 1 & (r < r_1) \\ \frac{r}{3[1+(r/r_O)^2]} & (r_1 < r < r_O) \\ M & (r > r_O) \end{cases},$$

$$f = \begin{cases} f_0 \left(1 - \frac{2}{r}\right) & (r < r_1) \\ \frac{c_0 r^2}{(1+3(r/r_O)^2)} & (r_1 < r < r_O) \\ 1 - \frac{2M}{r} & (r > r_O) \end{cases},$$

where

$$f_0 = \frac{8(1 + \beta^2)}{(3 + \beta^2)^2}, \quad c_0 = \frac{8}{3r_0^2}. \quad (4.3)$$

Here we set  $\beta \equiv r_O/r_1$ . The tangential pressure is given by

$$P_t = \frac{1 - (r/r_O)^2}{24\pi r^2 (1 + 3(r/r_O)^2)(1 + (r/r_O)^2)^2}.$$

The ISCO radius  $r_1$  is given by  $\beta$ , from the definition  $m(r_1) = 1$ , as

$$r_1 = 3 \left(1 + \frac{1}{\beta^2}\right).$$

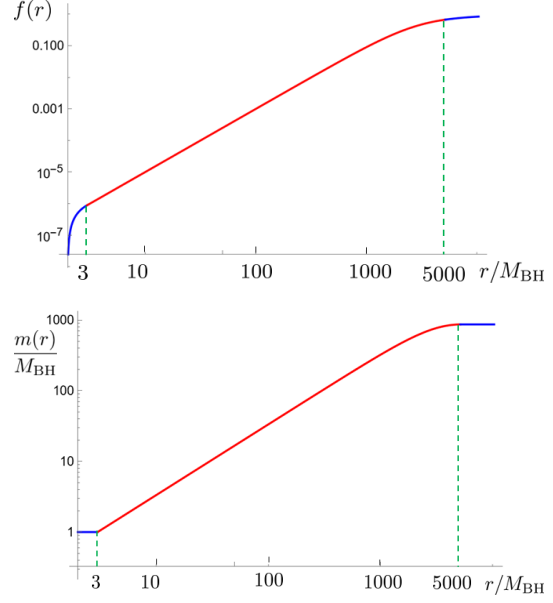


FIG. 4: Metric functions for Model II,  $f(r)$  (top) and  $m(r)$  (bottom). We set  $r_1 = 3.000001M_{\text{BH}}$ , which gives  $r_O = 5196.15M_{\text{BH}}$  and  $M_O = 866.0M_{\text{BH}}$ .

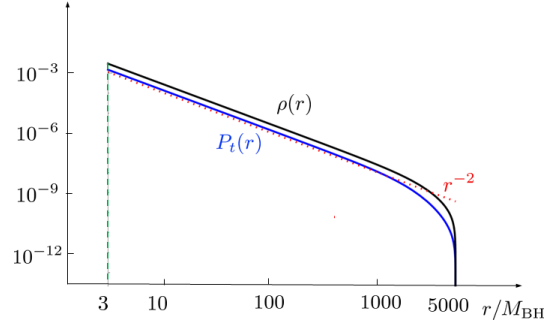


FIG. 5: The distributions of the energy density  $\rho$  and tangential pressure  $P_t$  for Model II. The parameters are the same as those in Fig. 4.

While the total mass  $M$  is also described by  $\beta$  as

$$M = m(r_O) = \frac{r_O}{6} = \frac{\beta r_1}{6} = \frac{1 + \beta^2}{2\beta}.$$

Since  $\beta > 1$ , we find  $3 < r_1 < 6$  and  $1 < M < \infty$ .

Expanding the mass function  $m(r)$  around  $r_1$ , we find

$$m(r) \approx 1 + \alpha(r - r_1) + O((r - r_1)^2),$$

where

$$\alpha = \frac{r_O^2(r_O^2 - r_1^2)}{3(r_O^2 + r_1^2)^2} = \frac{\beta^2(\beta^2 - 1)}{3(\beta^2 + 1)^2},$$

which satisfies  $0 < \alpha < 1/3$ . In the limit of  $\beta \rightarrow \infty$ , we find  $\alpha \rightarrow 1/3$ , i.e.,  $r_1 \rightarrow 3$  and  $M \rightarrow \infty$ .

We show the metric functions  $f(r)$  and  $m(r)$  of the present model in Fig. 4, and the energy density  $\rho$  and tangential pressure  $P_t$  in Fig. 5. We set  $\beta = 3$ , which gives  $r_I = 10/3$ ,  $r_O = 10$ , and  $M = 5/2$ .

### C. Model III

Finally, we find another simple analytic model. We assume the mass function  $m(r)$  as

$$m(r) = m_p r^p \quad (r_I \leq r \leq r_O), \quad (4.4)$$

where  $m_p$  and  $p(> 0)$  are some constants. The continuity of mass function at  $r_I$  is described by  $m(r_I) = m_p r_I^p = 1$ , and the condition of the ISCO,

$$r_I^2 m'(r_I) + r_{r m I} m(r_I) - 6m^2(r_I) = 0,$$

gives

$$(p+1)m_p r_I^{p+1} - 6m_p^2 r_I^{2p} = 0.$$

From these two conditions, we find

$$m_p = r_I^{-p}, \quad \text{and} \quad p = \frac{6 - r_I}{r_I}.$$

The condition of  $3 < r_I < 6$ , in which we are interested, gives  $0 < p < 1$ . The stability condition (3.2) gives

$$r \geq \left( \frac{6m_p}{p+1} \right)^{\frac{1}{1-p}} = r_I,$$

which is always satisfied.

The metric function should satisfy

$$\begin{aligned} \frac{1}{f} \frac{df}{dr} &= \frac{2m}{r(r-2m)} = \frac{2m_p r^{p-2}}{(1-2m_p r^{p-1})} \\ &= \frac{1}{1-p} \frac{d}{dr} \ln |(1-2m_p r^{p-1})|, \end{aligned}$$

which is integrated as

$$f = c_0 \left( 1 - \frac{2m_p}{r^{1-p}} \right)^{\frac{1}{1-p}},$$

where  $c_0$  is an integration constant.

With the continuity conditions at  $r = r_I$  and  $r_O$ , we find the metric functions as

$$m = \begin{cases} 1 & (r < r_I) \\ m_p r^p & (r_I < r < r_O), \\ M & (r > r_O) \end{cases}$$

$$f = \begin{cases} f_0 \left( 1 - \frac{2}{r} \right) & (2M < r < r_I) \\ c_0 \left( 1 - \frac{2m_p}{r^{1-p}} \right)^{\frac{1}{1-p}} & (r_I < r < r_O), \\ 1 - \frac{2M}{r} & (r > r_O) \end{cases}$$

where

$$c_0 = \left( 1 - \frac{2M}{r_O} \right) \left( 1 - \frac{2m_p}{r_O^{1-p}} \right)^{-\frac{1}{1-p}},$$

$$f_0 = \frac{\left( 1 - \frac{2M}{r_I} \right) \left[ \left( 1 - \frac{2m_p}{r_I^{1-p}} \right) \right]^{\frac{1}{1-p}}}{\left( 1 - \frac{2}{r_I} \right) \left[ \left( 1 - \frac{2m_p}{r_O^{1-p}} \right) \right]}.$$

In the present model, we have two free parameters,  $r_I$  and  $r_O$ , which should satisfy

$$\begin{aligned} 3 < r_I < 6, \\ r_O > r_I, \end{aligned}$$

which guarantees  $M > 1$ .  $\alpha$  is given by

$$\alpha = m'(r_I) = pm_p r_I^{p-1} = pm_p^{\frac{1}{p}} = \frac{6 - r_I}{r_I^2},$$

which gives

$$0 < \alpha < \frac{1}{3}.$$

The energy density is given by

$$\rho = \frac{m'}{4\pi r^2} = \frac{6 - r_I}{4\pi r_I^{p+1}} r^{3-p}.$$

The power exponent of density distribution  $(3-p)$  is uniform and its value takes between 2 and 3.

We just show one example in Figs. 6 and 7.

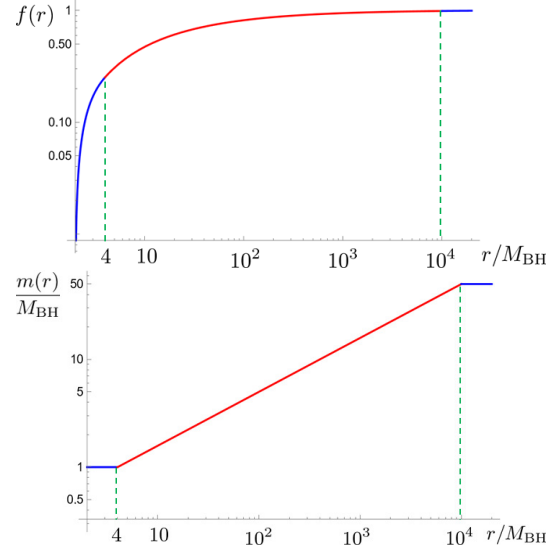


FIG. 6: Metric functions for Model III,  $f(r)$  (top) and  $m(r)$  (bottom). We set  $r_I = 4M_{\text{BH}}$  ( $p = 0.5$ ) and  $r_O = 10^4 M_{\text{BH}}$ , which gives  $50M_{\text{BH}}$ .

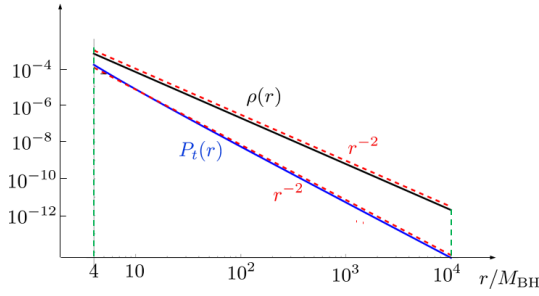


FIG. 7: The energy density  $\rho$  and tangential pressure  $P_t$  for Model III. The parameters are the same as those in Fig.6.

This model can be extended to the similar mass function such that

$$m = \frac{m_p r^p}{1 + (r_*/r)^{(1-p)}}, \quad (4.5)$$

with  $0 < p < 1$ . The metric function is

$$f = c_0 \left[ 1 - \frac{2m_p - r_*^{1-p}}{r^{1-p}} \right]^q, \quad (4.6)$$

where

$$q = \frac{1}{(1-p) \left[ 1 - r_*^{1-p}/(2m_p) \right]}.$$

For  $r_* = 0$ , we recover the previous model. The energy density is given by

$$\rho = \frac{m'}{4\pi r^2} = \frac{pm_p}{4\pi r^{3-p}} \frac{1 + \frac{2-p}{p} \left(\frac{r_*}{r}\right)^{1-p}}{\left[1 + \left(\frac{r_*}{r}\right)^{1-p}\right]^2}. \quad (4.7)$$

For  $r > r_*$ , the density distribution is almost the same as the previous model, i.e.,  $\gamma = 3 - p$ . In the range of  $r < r_*$ , the power exponent of the density distribution becomes  $\gamma = 2$ .

#### D. Comparison of the three models

We summarize the three toy models in Table I. For Models I and III,  $m(r) \rightarrow \infty$  as  $r \rightarrow \infty$ . Hence we have to terminate the distribution at a finite radius  $r_O$ . Here we set  $r_O = 10^4 M_{\text{BH}}$ . As examples, the ISCO radii are chosen as  $r_I = 5.5 M_{\text{BH}}$ ,  $4 M_{\text{BH}}$  and  $3 M_{\text{BH}}$  (or a value close to it if not possible).

Model	$r_I/M_{\text{BH}}$	$r_O/M_{\text{BH}}$	$M/M_{\text{BH}}$	$M/r_O$	$\gamma$	properties
I	5.5	10000	166.2	0.0166	2	isothermal stable (marginally stable)
	4		1250.5	0.125		
	3		3333.3	0.333		
II	5.5	6.025	1.00416	0.1667	12 ( $\rightarrow \infty$ )	marginally stable too small $r_O$ except for $r_I \approx 3$
	4	6.928	1.1547	0.1667	4 ( $\rightarrow \infty$ )	
	3.001	164.4	27.4	0.1667	2 ( $\rightarrow \infty$ )	
	3.000001	5196.15	866.0	0.1667	2 ( $\rightarrow \infty$ )	
III	$5.5 (p = \frac{1}{11})$	10000	42.6	0.00426	2.5	stable too small mass $M$
	$4 (p = \frac{1}{2})$		50	0.005		
	$3 (p = 1)$		57.7	0.00577		

TABLE I: Typical values of parameters in three toy models (I, II, and III). For Model I and III, we choose  $r_O = 10^4 M_{\text{BH}}$ , while the radius  $r_O$  of Model II is fixed. The power exponent of the density distribution is defined by  $\gamma = -\frac{d \ln \rho}{d \ln r}$ . In Model II, the density drops rapidly near the outer boundary  $r_O$ .

#### V. SOME REALISTIC MODEL

Although we do not know the exact DM distribution for any galaxy, a general feature is

the existence of some characteristic galactic scale, where the power exponent  $\gamma$  of the distribution changes [23–25]. This scale is much larger than the SMBH horizon scale. Hence we consider some model with a typical scale length much larger than

the horizon.

To model realistic DM distributions more closely, we consider the following model with mass function

$$m(r) = \frac{m_0 + m_1 r + Mr^2}{(r + r_*)^2}, \quad (5.1)$$

where  $m_0, m_1$ , and  $M$  are some constants. We call it Model IV.

Inside  $r_I$  is a vacuum and there exists a BH with the mass  $M_{\text{BH}} = 1$ . From the continuity of the mass function  $m(r)$ , we find  $m(r_I) = 1$ . The inner boundary  $r_I$  is assumed to be the ISCO radius, which satisfies

$$r_I^2 m'(r_I) + r_I m(r_I) - 6m^2(r_I) = 0,$$

with

$$m'(r) = \frac{m_1 r_* - 2m_0 + (2Mr_* - m_1)r}{(r + r_*)^3}. \quad (5.2)$$

---

For Einstein cluster, since  $L^2 > 0$  and  $E^2 > 0$ , we have the constraint of  $r > 3m(r)$ . The stability condition (3.2) should be also satisfied. Hence we have two constraints, which are described as

$$C_1(r) \equiv r^3 + (2r_* - 3M)r^2 + (r_*^2 - 3m_1)r - 3m_0 > 0, \quad (5.7)$$

$$C_2(r) \equiv Mr^5 + 2M(2r_* - 3M)r^4 + (3Mr_*^2 + 2m_1 r_* - 12m_1 M - m_0)r^3 - 2(6m_0 M + 3m_1^2 - m_1 r_*^2)r^2 + m_0(r_*^2 - 12m_1)r - 6m_0^2 \geq 0. \quad (5.8)$$

These constraints should be satisfied in the whole range of distribution ( $r_I \leq r \leq r_O$ ). This restricts the parameter range of  $r_*$  and  $r_I$  (and  $M$  if it is not fixed). Note that those constraints are satisfied at  $r_I$  as

$$C_1(r_I) = (r_I - 3)(r_I + r_*)^2 > 0, \quad C_2(r_I) = 0,$$

because  $r_I > 3$ . Since  $C_2(r)$  vanishes at  $r_I$ , we can factorise it with  $(r - r_I)$  by use of Eqs. (5.5) and (5.6). Hence setting  $C_2(r) = (r - r_I)\tilde{C}_2(r)$ , the constraint with  $C_2(r)$  is reduced to a quartic inequality i.e.,

$$\tilde{C}_2(r) \geq 0, \quad (5.9)$$

where

$$\begin{aligned} \tilde{C}_2(r) \equiv & Mr^4 - M(6M - 4r_* - r_I)r^3 \\ & + \frac{1}{r_I^2} [6(r_* + r_I)^2(2r_* + r_I) - 2r_*^2 r_I(r_* + r_I) + 18M^2 r_I^3 - 3M(24(r_* + r_I)^2 - 4r_I(r_*^2 - r_I^2) - r_*^2 r_I^2)] r^2 \\ & - \frac{1}{r_I^4} [6(r_* + r_I)^2 - 2r_* r_I(r_* + r_I) - Mr_I^3] [36(r_* + r_I)^2 + 12r_I^2(r_* + r_I) - r_*^2 r_I^2 - 18Mr_I^3] r \\ & + \frac{6}{r_I^3} [6(r_* + r_I)^2 - 2r_* r_I(r_* + r_I) - Mr_I^3]^2. \end{aligned} \quad (5.10)$$

The energy density  $\rho$  is

$$\rho = \frac{m'}{4\pi r^2} = \frac{m_1 r_* - 2m_0 + (2Mr_* - m_1)r}{4\pi r^2 (r + r_*)^3}.$$

The above two conditions give

$$m_0 + m_1 r_I + Mr_I^2 = (r_I + r_*)^2 \quad (5.3)$$

$$\begin{aligned} r_I^2 [m_1 r_* - 2m_0 + (2Mr_* - m_1)r_I] \\ = (6 - r_I)(r_I + r_*)^3, \end{aligned} \quad (5.4)$$

which solve  $m_0$  and  $m_1$  as

$$m_0 = Mr_I^2 + \frac{2(r_* + r_I)}{r_I} [(r_I - 3)r_* - 3r_I], \quad (5.5)$$

$$m_1 = \frac{(r_* + r_I)}{r_I^2} [(6 - r_I)r_* + (6 + r_I)r_I] - 2Mr_I. \quad (5.6)$$

---

From the condition (5.4), we find  $r_I \leq 6$  because  $\rho(r_I) \geq 0$ . If  $\rho(r_I) = 0$ , we find  $r_I = 6$ , which is the BH ISCO radius. Since we are interested in the case of  $r_I < 6$ , the energy density does not vanish



at  $r_I$ .

The metric function  $f$  is obtained as

$$f = f_0 \exp I(r), \quad (5.11)$$

where  $f_0 = f(r_I)$  is an integration constant and  $I(r)$  is defined by the integration

$$\begin{aligned} I(r) &\equiv \int_{r_I}^r dr \frac{2m(r)}{r(r-2m(r))} \\ &= \int_{r_I}^r dr \frac{2(m_0 + m_1 r + Mr^2)}{r[r(r+r_*)^2 - 2(m_0 + m_1 r + Mr^2)]}, \end{aligned}$$

which analytic solutions are given in Appendix A. For the models we consider here, the metric function  $f(r)$  is always finite in the whole range.

From the density distribution, we can classify this model into two cases.

- Type A :  $m_1 r_* - 2m_0 = 0$   
Since the density must be positive,  $(2Mr_* - m_1)$  is positive.
- Type B :  $m_1 r_* - 2m_0 \neq 0$   
This type is further classified into three cases as

- \* Type B<sub>+</sub> :  $2Mr_* - m_1 > 0$
- \* Type B<sub>0</sub> :  $2Mr_* - m_1 = 0$
- \* Type B<sub>-</sub> :  $2Mr_* - m_1 < 0$

In the last two cases,  $(m_1 r_* - 2m_0)$  must be positive. Since the density vanishes at a finite radius in Type B<sub>-</sub>, the radius of the distribution must be finite.

We shall discuss these types separately in below.

### A. Type A

In the case of  $m_1 r_* - 2m_0 = 0$ , there are two free parameters  $r_*$  and  $r_I$ . The other parameters  $m_0, m_1, M$  are fixed as

$$m_0 = \frac{r_*}{2r_I} [3(r_I - 2)r_* - (6 - r_I)r_I], \quad (5.12)$$

$$m_1 = \frac{1}{r_I} [3(r_I - 2)r_* - (6 - r_I)r_I], \quad (5.13)$$

$$M = 1 + \frac{(6 - r_I)}{2r_I^3} (r_* + r_I)(r_* + 2r_I). \quad (5.14)$$

The density distribution is

$$\rho = \frac{2Mr_* - m_1}{4\pi r(r+r_*)^3},$$

which is the Hernquist type distribution, i.e.,  $\rho \propto r^{-\gamma}$  with  $\gamma = 1$  for  $r < r_*$  while  $\gamma = 4$  for  $r > r_*$ .

Since  $M > 1 (= M_{\text{BH}})$ ,  $r_I < 6$ . The condition of  $2Mr_* - m_1 > 0$  gives

$$C_3 \equiv (6 - r_I)(r_* + r_I)^3 - 2r_* r_I^3 > 0.$$

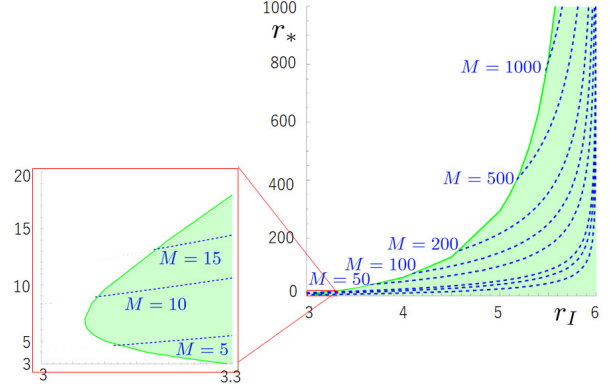


FIG. 8: The existence range of solutions of Type A in the  $r_I$ - $r_*$  plane. The left panel is the enlarged one of the left-bottom corner. The blue dotted curves are contours of mass  $M$ .

As we discussed, we have two more constraints on  $r_*$  and  $r_I$  by  $C_1(r) > 0$  and  $\tilde{C}_2(r) > 0$  since  $M$  is given by Eq. (5.14). These three constraints restrict the parameter range of  $r_*$  and  $r_I$ . We show it by the lightgreen region in Fig. 8. For larger values of  $r_*$ , the existence region in  $r_I$  becomes smaller and  $r_I \rightarrow 6$  as  $r_* \rightarrow \infty$ .

Since  $M$  is the total mass of a galaxy, the scale of the gravitational potential is  $M/r_*$ , which is given by

$$\frac{M}{r_*} = \frac{1}{r_*} \left[ 1 + \frac{(6 - r_I)}{2r_I^3} (r_* + r_I)(r_* + 2r_I) \right].$$

It is approximated as

$$\frac{M}{r_*} \sim \frac{(6 - r_I)}{2r_I^3},$$

when  $r_* \gg 1$ .

### B. Type B<sub>0</sub>

In the case of  $2Mr_* - m_1 = 0$ , there are also two free parameters  $r_*$  and  $r_I$ . The other parameters

$m_0, m_1, M$  are fixed as

$$m_0 = \frac{2r_*^2(r_I - 3)}{r_I} - \frac{1}{2}(6 - r_I)(3r_* + r_I), \quad (5.15)$$

$$m_1 = \frac{r_*}{r_I^2} [(6 - r_I)r_* + (6 + r_I)r_I], \quad (5.16)$$

$$M = \frac{1}{2r_I^2} [(6 - r_I)r_* + (6 + r_I)r_I]. \quad (5.17)$$

Since

$$m_1 r_* - 2m_0 = \frac{(6 - r_I)(r_* + r_I)^3}{r_I^2} > 0, \quad (5.18)$$

when  $r_I < 6$ , we have two constraints on  $r_*$  and  $r_I$  by  $C_1(r) > 0$  and  $\tilde{C}_2(r) > 0$ . These constraints restrict the parameter range of  $r_*$  and  $r_I$ . We show it by the lightgreen region in Fig. 9.

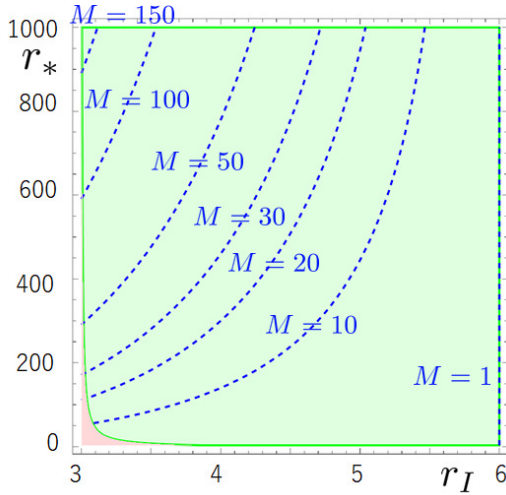


FIG. 9: The existence range Type B<sub>0</sub> of solutions in the  $r_I$ - $r_*$  plane. The blue dotted curves are contours of mass  $M$ .

The energy density is given by

$$\rho = \frac{m'}{4\pi r^2} = \frac{m_1 r_* - 2m_0}{4\pi r^2 (r + r_*)^3},$$

i.e.,  $\rho \propto r^{-\gamma}$  with  $\gamma = 2$  for  $r < r_*$  while  $\gamma = 5$  for  $r > r_*$ .

### C. Type B<sub>±</sub>

In Type B<sub>±</sub>, three parameters ( $r_*$ ,  $r_I$ , and  $M$ ) are free. The other parameters ( $m_0, m_1$ ) are fixed by (5.5) and (5.6). The condition of  $2Mr_* - m_1 \geq 0$  gives the constraint on  $M$  as

$$M \geq \frac{1}{2r_I^2} [(6 - r_I)r_* + (6 + r_I)r_I].$$

With this constraint, two additional constraints (5.7) and (5.9) give the constraint on  $M$  for given values of  $r_I$  and  $r_*$ . In Fig. 10, we show the existence region of solutions for given values of  $r_* = 10^2, 10^3$  and  $10^4$ . The solutions of Type B<sub>+</sub> exist in the lightgreen region in Fig. 10. The energy density extends to infinity. The density profile is  $\rho \propto r^{-\gamma}$  with  $\gamma = 2$  for  $r < r_*$  while  $\gamma = 4$  for  $r > r_*$ .

While, for Type B<sub>-</sub>, the solutions exist in the green region in Fig. 10. The energy density vanishes at finite radius  $r_O$ , which is

$$\begin{aligned} r_O &= \frac{m_1 r_* - 2m_0}{2Mr_* - m_1} \\ &= \frac{[(6 - r_I)r_*^2 + 3(6 - r_I)r_I r_* + 12r_I^2] - 2Mr_I^3}{[(6 - r_I)r_* + (6 + r_I)r_I - 2Mr_I^2]}. \end{aligned}$$

It should be the outer boundary of DM distribution. The total mass of a galaxy is

$$m(r_O) = \frac{m_0 + m_1 r_O + Mr_O^2}{(r_O + r_*)^2} = M_G. \quad (5.19)$$

The density profile is  $\rho \propto r^{-\gamma}$  with  $\gamma = 2$  for  $r < r_*$  while  $\gamma = 5$  for  $r > r_*$ . However the outer boundary  $r_O$  is almost same as  $r_*$  when  $r_* \gg 1$ . As a result  $\gamma$  is indefinite near the boundary.

Note that the solution of Type B<sub>0</sub> exists at the boundary between two types, B<sub>+</sub> and B<sub>-</sub>. The solution of Type A is also a special limit in Type B<sub>+</sub>, which is shown by the red curve.

### D. Typical values of Model IV and density distributions

In Table II, we summarize the typical values of Model IV. We choose  $r_I = 5.5M_{\text{BH}}, 4M_{\text{BH}}$  and  $3M_{\text{BH}}$  (or a value close to it if not possible). In Type A, since  $r_*$  is bounded above, we choose the maximum

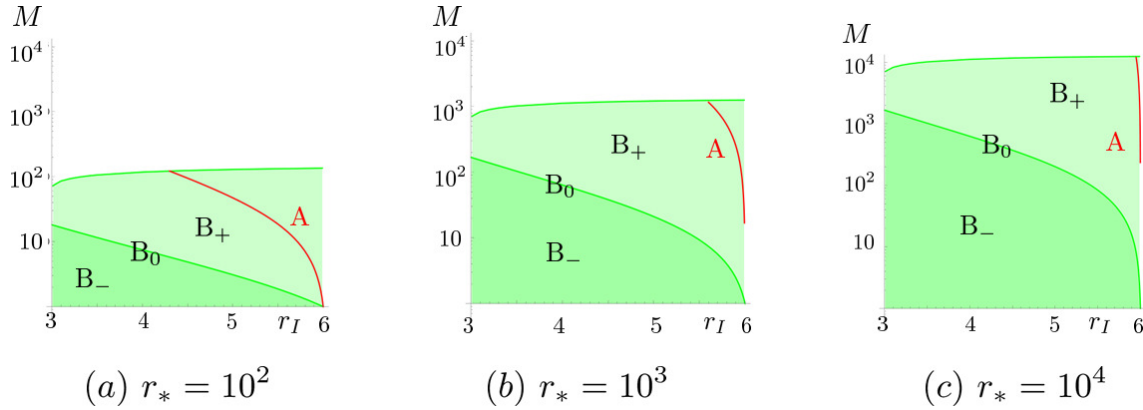


FIG. 10: The existence range of solutions in the  $r_I$ - $M$  plane for Model IV. The solutions of Type  $B_+$  and Type  $B_-$  exist in the lightgreen and green regions, respectively. We choose (a)  $r_* = 10^2$ , (b)  $r_* = 10^3$ , and (c)  $r_* = 10^4$ . The solutions of Type  $B_0$  are found at the boundary. The solutions of Type A (the red curve) appear as a special limit of Type  $B_+$ .

Type	$r_I/M_{\text{BH}}$	$r_*/M_{\text{BH}}$	$r_O/M_{\text{BH}}$	$M/M_{\text{BH}}$	$M/r_*$	$M/r_O$	$\gamma$	DM distribution
A	5.5	808	$\infty$	1002.1	1.240	0	$1 \rightarrow 4$	Hernquist profile
	4	64		77.5	1.211			
	3.069	6.9		7.59	1.100			
$B_0$	5.5	10000	$\infty$	83.69	0.008369	0	$2 \rightarrow 5$	infinite radius
	4			626.25	0.062625			
	3			1668.17	0.166817			
$B_+$	5.5	10000	$\infty$	90	0.009	0	$2 \rightarrow 4$	infinite radius
	4			700	0.07			
	3			1800	0.18			
$B_-$	5.5	10000	$1.2 \times 10^6$	83	0.0083	$6.92 \times 10^{-5}$	$2 \rightarrow 5$	finite radius
	4		$2.5 \times 10^7$	626	0.0626	$2.5 \times 10^{-5}$		
	3		$1.0 \times 10^8$	1668	0.1668	$1.67 \times 10^{-5}$		

TABLE II: Typical values of parameters in Model IV. The scale length of DM distribution is chosen as  $r_* = 10^4 M_{\text{BH}}$ .

values for given  $r_I$ . We also choose  $r_I = 3.069 M_{\text{BH}}$ , which is the minimum possible value. For Type B, the scale length of DM distribution is chosen as  $r_* = 10^4 M_{\text{BH}}$ . For the masses of Type  $B_+$  and Type  $B_-$ , we choose a slightly larger and smaller values than the mass of Type  $B_0$ , respectively.

In Figs. 11, we show the density distributions for these models in Table II. We choose  $r_I = 4 M_{\text{BH}}$ . The power exponent  $\gamma$  changes from 1 to 4 for Type A, from 2 to 5 for Type  $B_0$ , from 2 to 4 for Type  $B_+$ , and from 2 to 5 for Type  $B_-$ , respectively. For Type  $B_-$ , the power exponent  $\gamma$  diverges near the outer boundary because the density vanishes rapidly there.

In Fig. 12, we also show the mass functions  $m(r)$  for the same models.

As for the metric function  $f(r)$ , we find that the solution exists in whole range of  $r_I \leq r < \infty$  ( $r_I \leq r < r_O$  for Type  $B_-$ ). The three roots (see Appendix for the meaning of the three roots) are

Type A :  $(1.555, 12.72 \pm 60.88 i)$  [case (2)]

Type  $B_0$ :  $(-12967., -5782., 1.33298)$  [case (1-1)]

Type  $B_+$ :  $(-12696., -5906., 1.33299)$  [case (1-1)]

Type  $B_-$ :  $(-12968., -5782., 1.33298)$  [case (1-1)]

Using these three roots, we depict the metric functions  $f$  for the same models in Fig. 13.

From these figures, we find three types  $B_0$  and  $B_{\pm}$  are very similar because the parameters we choose in  $B_{\pm}$  are very close to those in  $B_0$ . If we choose them far from  $B_0$ , we find the different distributions. The behaviours of Type A are also very different from those of Type B.

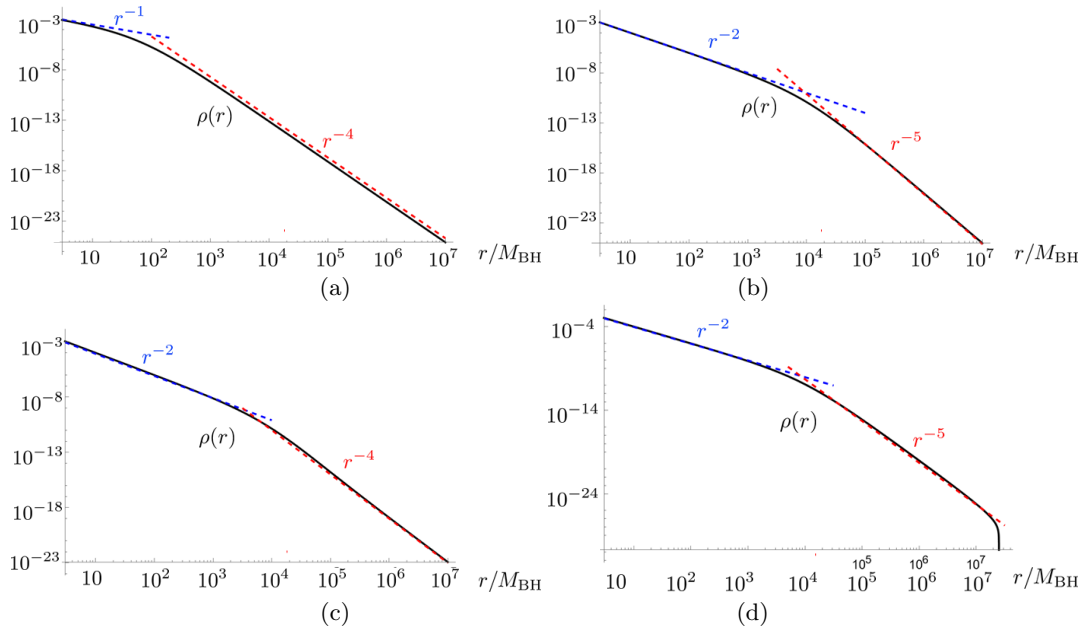


FIG. 11: The density distributions of (a) Type A, (b) Type B<sub>0</sub>, (c) Type B<sub>+</sub>, and (d) Type B<sub>-</sub>. We choose  $r_1 = 4M_{\text{BH}}$ .

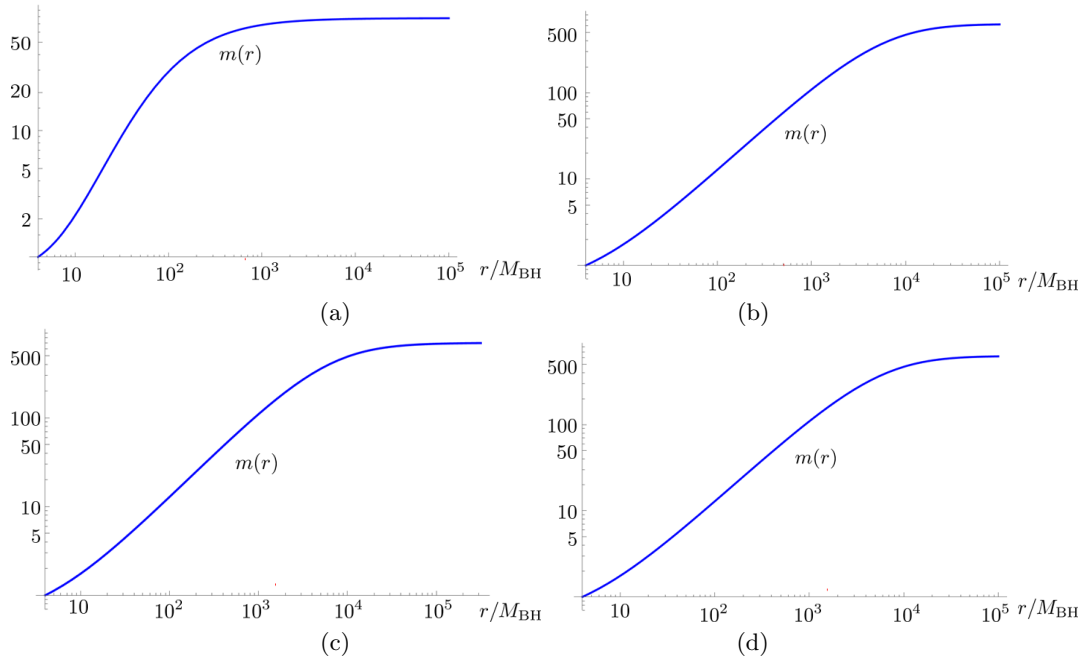


FIG. 12: The mass functions of (a) Type A, (b) Type B<sub>0</sub>, (c) Type B<sub>+</sub>, and (d) Type B<sub>-</sub>. We choose  $r_1 = 4M_{\text{BH}}$ .

## VI. SUMMARY AND REMARKS

Using the Einstein cluster model, we discuss general relativistic solutions describing possible BH environments. In particular, we show that nontrivial distributions can occur the (isolated) BH ISCO radius ( $6M_{\text{BH}}$ ). We have presented simple, real-

istic models with a specific galactic scale, as well as three toy models. The ISCO radius of the matter distribution is found to lie between the photon radius ( $3M_{\text{BH}}$ ) and the BH ISCO radius.

One of the issues that we don't address is stability of these configurations. There have been discussions regarding the stability of the Einstein

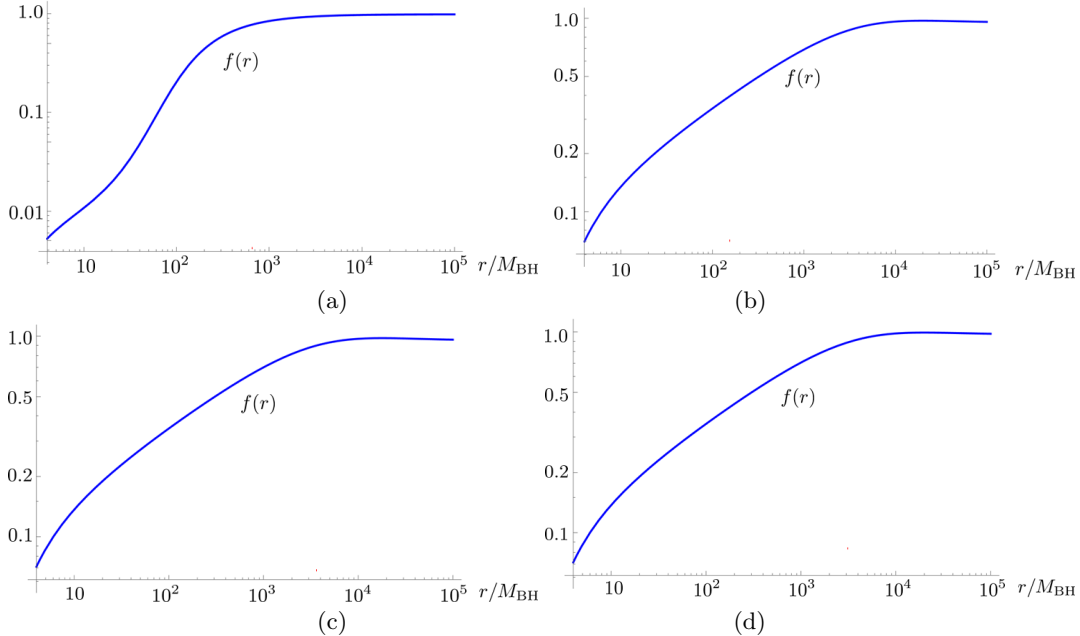


FIG. 13: The metric functions  $f$  of (a) Type A, (b) Type B<sub>0</sub>, (c) Type B<sub>+</sub>, and (d) Type B<sub>-</sub>. We choose  $r_1 = 4M_{\text{BH}}$ .

clusters [22, 26]. The Einstein cluster under our stability condition (3.2) appears to be metastable in the range of  $3m(r) < r < 6m(r)$ , and it may become unstable when we consider a simple Einstein cluster star[26]. However there exists a BH inside the matter distribution in our models, and most of DM distribution satisfies the absolute stability condition ( $r > 6m(r)$ ) including the region outside the DM distribution. Therefore, we must carefully reanalyze the stability of such a system.

The presence of matter in such a strong gravity region may be significant for gravitational wave observations, as well as for the DM search experiments, such as those involving particle annihilation or creation. We will leave these important studies, along with the stability analysis, for future work.

### Acknowledgments

We thank Robin Diedrichs and Tomohiro Harada for useful discussions. We would like to acknowledge the Yukawa Institute for Theoretical Physics at Kyoto University, where the present work was begun during the YITP long-term workshop, Gravity and Cosmology 2024. KM would also thank Institute for Theoretical Physics and Cosmology, Zhejiang University of Technology and Niels Bohr Institute/Niels Bohr International Academy, where this work was completed. This work was supported in part by JSPS KAKENHI

Grant Number JP24K07058. V.C. is a Villum Investigator and a DNRF Chair. V.C. acknowledges financial support provided under the European Union’s H2020 ERC Advanced Grant “Black holes: gravitational engines of discovery” grant agreement no. Gravitas–101052587. Views and opinions expressed are however those of the author only and do not necessarily reflect those of the European Union or the European Research Council. Neither the European Union nor the granting authority can be held responsible for them. This project has received funding from the European Union’s Horizon 2020 research and innovation programme under the Marie Skłodowska-Curie grant agreement No 101007855 and No 101131233. We acknowledge support by VILLUM Foundation (grant no. VIL37766) and the DNRF Chair program (grant no. DNRF162) by the Danish National Research Foundation. A.W. is partially supported by the US NSF grant: PHY-2308845.

**Appendix A: The metric function  $f(r)$  in Model IV**

In this appendix, we integrate the metric function  $f(r)$ . The metric function  $f$  is given by

$$f = f_0 \exp I(r), \quad (\text{A1})$$

with

$$I(r) = \int_{r_1}^r dr \frac{2(m_0 + m_1 r + Mr^2)}{r[r(r+r_*)^2 - 2(m_0 + m_1 r + Mr^2)]}. \quad (\text{1-3}) \quad (r_1 < r_2 = r_3)$$

In order integrate it, we first consider the cubic equation  $p(r) \equiv r(r+r_*)^2 - 2(m_0 + m_1 r + Mr^2) = 0$ . It may contain three real roots,  $r_1, r_2, r_3$  ( $r_1 \leq r_2 \leq r_3$ ) (case 1), or one real root  $r_1$  and two complex conjugate roots  $\xi \pm i\eta$  (case 2).

(1-1) three different real roots ( $r_1 < r_2 < r_3$ )

In this case, we find

$$I(r) = \ln [r^a (r - r_1)^b (r - r_2)^c (r - r_3)^d],$$

where

$$\begin{aligned} a &= -\frac{2m_0}{r_1 r_2 r_3}, \\ b &= \frac{2[m_0 + r_1(m_1 - Mr_1)]}{r_1(r_2 - r_1)(r_3 - r_1)}, \\ c &= -\frac{2[m_0 + r_2(m_1 - Mr_2)]}{r_2(r_2 - r_1)(r_3 - r_2)}, \\ d &= \frac{2[m_0 + r_3(m_1 - Mr_3)]}{r_3(r_3 - r_1)(r_3 - r_2)}. \end{aligned}$$

Hence the metric function is given by

$$f(r) = f_0 r^a (r - r_1)^b (r - r_2)^c (r - r_3)^d. \quad (\text{A2})$$

Since  $a + b + c + d = 0$ ,  $f$  approaches a constant as  $r \rightarrow \infty$ . However, if at least one of  $r_i$  ( $i = 1, 2, 3$ ) is larger than  $r_I$ ,  $f$  will diverges at that point. The solution cannot be extended further.

(1-2) ( $r_1 = r_2 < r_3$ )

$$I(r) = a \ln r + b \ln(r - r_1) - \frac{c}{(r - r_1)} + d \ln(r - r_3),$$

where

$$\begin{aligned} a &= -\frac{2m_0}{r_1^2 r_3}, \\ b &= \frac{2[m_0(2r_1 - r_3) + (m_1 + Mr_3)r_1^2]}{r_1^2(r_3 - r_1)^2}, \\ c &= -\frac{2[m_0 + r_1(m_1 + Mr_1)]}{r_1(r_3 - r_1)}, \\ d &= \frac{2[m_0 + r_3(m_1 + Mr_3)]}{r_3(r_3 - r_1)^2}. \end{aligned}$$

Hence the metric function is given by

$$f(r) = f_0 r^a (r - r_1)^b (r - r_3)^d \exp \left[ -\frac{c}{(r - r_1)} \right]. \quad (\text{A3})$$

Since  $a + b + d = 0$ ,  $f$  approaches a constant as  $r \rightarrow \infty$ . However, if at least one of  $r_i$  ( $i = 1, 3$ ) is larger than  $r_I$ ,  $f$  will diverges at that point. The solution cannot be extended further.

$$I(r) = a \ln r + b \ln(r - r_1) + c \ln(r - r_2) - \frac{d}{(r - r_2)},$$

where

$$\begin{aligned} a &= -\frac{2m_0}{r_1 r_2^2}, \\ b &= \frac{2[m_0 + (m_1 + Mr_1)r_1]}{r_1(r_2 - r_1)^2}, \\ c &= -\frac{2[m_0(-r_1 + 2r_2) + m_1 r_2^2 + Mr_1 r_2^2]}{r_2^2(r_2 - r_1)^2}, \\ d &= \frac{2[m_0 + (m_1 + Mr_2)r_2]}{r_2(r_2 - r_1)}. \end{aligned}$$

Hence the metric function is given by

$$f(r) = f_0 r^a (r - r_1)^b (r - r_2)^c \exp \left[ -\frac{d}{(r - r_2)} \right]. \quad (\text{A4})$$

Since  $a + b + c = 0$ ,  $f$  approaches a constant as  $r \rightarrow \infty$ . However, if at least one of  $r_i$  ( $i = 1, 2$ ) is larger than  $r_I$ ,  $f$  will diverges at that point. The solution cannot be extended further.

(1-4) ( $r_1 = r_2 = r_3$ )

$$I(r) = a \ln r + b \ln(r - r_1) - \frac{c}{(r - r_1)} - \frac{d}{2(r - r_1)^2},$$

where

$$\begin{aligned} a &= -\frac{2m_0}{r_1^3}, \\ b &= \frac{2m_0}{r_1^3}, \\ c &= \frac{2[-m_0 + Mr_1^2]}{r_1^2}, \\ d &= \frac{2[m_0 + (m_1 + Mr_1)r_1]}{r_1}. \end{aligned}$$

Hence the metric function is given by

$$f(r) = f_0 r^a (r - r_1)^b \exp \left[ -\frac{c}{(r - r_1)} - \frac{d}{2(r - r_1)^2} \right] \quad (\text{A5})$$

Since  $a+b=0$ ,  $f$  approaches a constant as  $r \rightarrow \infty$ . However, if  $r_1$  is larger than  $r_I$ ,  $f$  will diverges at that point. The solution cannot be extended further.

(2) one real root and two complex conjugate roots

In this case, the integrand is given as

$$\frac{a}{r} + \frac{b}{r-r_1} + \frac{\gamma r + \delta}{r^2 - 2\xi r + \xi^2 + \eta^2},$$

where

$$\begin{aligned} a &= -\frac{2m_0}{r_1(\xi^2 + \eta^2)}, \\ b &= \frac{2(m_0 + m_1 r_1 + M r_1^2)}{r_1(r_1^2 - 2r_1 \xi + \xi^2 + \eta^2)}, \\ \gamma &= -\frac{2[(-m_0 + M(\xi^2 + \eta^2))r_1 + 2m_0 \xi + m_1(\xi^2 + \eta^2)]}{(\xi^2 + \eta^2)(r_1^2 - 2r_1 \xi + \xi^2 + \eta^2)}, \\ \delta &= \frac{2[-(2m_0 \xi + m_1(\xi^2 + \eta^2))r_1 + m_0(3\xi^2 - \eta^2) + 2m_1 \xi(\xi^2 + \eta^2) + M(\xi^2 + \eta^2)^2]}{(\xi^2 + \eta^2)(r_1^2 - 2r_1 \xi + \xi^2 + \eta^2)}. \end{aligned}$$

We then find

$$I(r) = a \ln r + b \ln(r - r_1) + \frac{\gamma}{2} \ln(r^2 - 2\xi r + \xi^2 + \eta^2) + \frac{(\gamma \xi + \delta)}{\eta} \arctan \left[ \frac{(r - \xi)}{\eta} \right].$$

Hence the metric function is given by

$$f(r) = f_0 r^a (r - r_1)^b (r^2 - 2\xi r + \xi^2 + \eta^2)^{\gamma/2} \exp \left[ \frac{(\gamma \xi + \delta)}{\eta} \arctan \left[ \frac{(r - \xi)}{\eta} \right] \right]. \quad (\text{A6})$$

Since  $a+b+\gamma=0$ ,  $f$  approaches a constant as  $r \rightarrow \infty$ . We also find  $r_1$  is always smaller than  $r_I$  because  $p(r_1) = r_1(r_1 + r_*)^2 - 2(m_0 + m_1 r_1 + M r_1^2) = (r_1 - 2)(r_1 + r_*)^2 > 0$ . Hence  $f$  does not diverge anywhere.

- 
- [1] K. Freese, EAS Publ. Ser. **36**, 113 (2009), 0812.4005.
- [2] J. F. Navarro, C. S. Frenk, and S. D. M. White, *Astrophys. J.* **462**, 563 (1996), astro-ph/9508025.
- [3] D. Clowe, M. Bradac, A. H. Gonzalez, M. Markevitch, S. W. Randall, C. Jones, and D. Zaritsky, *Astrophys. J. Lett.* **648**, L109 (2006), astro-ph/0608407.
- [4] G. Bertone, D. Hooper, and J. Silk, *Phys. Rept.* **405**, 279 (2005), hep-ph/0404175.
- [5] F. Kahlhoefer, *Int. J. Mod. Phys. A* **32**, 1730006 (2017), 1702.02430.
- [6] C. Pérez de los Heros, *Symmetry* **12**, 1648 (2020), 2008.11561.
- [7] P. Gondolo and J. Silk, *Phys. Rev. Lett.* **83**, 1719 (1999), arXiv:astro-ph/9906391.
- [8] K. Eda, Y. Itoh, S. Kuroyanagi, and J. Silk, *Phys. Rev. D* **91**, 044045 (2015).
- [9] V. Cardoso, K. Destounis, F. Duque, R. P. Macedo, and A. Maselli, *Phys. Rev. D* **105**, L061501 (2022), arXiv:2109.00005.
- [10] F. Duque, C. F. B. Macedo, R. Vicente, and V. Cardoso (2023), 2312.06767.
- [11] A. M. Ghez, S. Salim, N. N. Weinberg, J. R. Lu, T. Do, J. K. Dunn, K. Matthews, M. R. Morris, S. Yelda, E. E. Becklin, et al., *Astrophys. J.* **689**, 1044 (2008), 0808.2870.
- [12] GRAVITY Collaboration, R. Abuter, A. Amorim, M. Bauböck, J. P. Berger, H. Bonnet, W. Brandner, Y. Clénet, V. Coudé Du Foresto, P. T. de Zeeuw, et al., *Astron. Astrophys.* **625**, L10 (2019), 1904.05721.
- [13] R. Abuter et al. (GRAVITY), *Astron. Astrophys.* **657**, L12 (2022), 2112.07478.
- [14] T. Igata, T. Harada, H. Saida, and Y. Takamori, *Int. J. Mod. Phys. D* **32**, 2350105 (2023), arXiv:2202.00202.
- [15] L. Hernquist, *The Astrophysical Journal* **356**, 359

- (1990).
- [16] F. Ferrer, A. M. da Rosa, and C. M. Will, *Phys. Rev. D* **96**, 083014 (2017), arXiv:1707.06302.
  - [17] N. Speeney, E. Berti, V. Cardoso, and A. Maselli, *Phys. Rev. D* **109**, 084068 (2024), 2401.00932.
  - [18] Z. Shen, A. Wang, and S. Yin (2024), arXiv:2408.05417.
  - [19] Z. Shen, A. Wang, Y. Gong, and S. Yin, *Phys. Lett. B* **855**, 138797 (2024), 2311.12259.
  - [20] C. G. Bohmer and T. Harko, *Monthly Notices of the Royal Astronomical Society* **379**, 393 (2007).
  - [21] K. Jusufi, *The European Physical Journal C* **83**, 103 (2023).
  - [22] R. Acharyya, P. Banerjee, and S. Kar (2023), arXiv:2311.18622.
  - [23] D. J. Sand, T. Treu, G. P. Smith, and R. S. Ellis, *The Astrophysical Journal* **604**, 88 (2004).
  - [24] A. Borriello and P. Salucci, *Mon. Not. Roy. Astron. Soc.* **323**, 285 (2001), astro-ph/0001082.
  - [25] P. Salucci, *Astron. Astrophys. Rev.* **27**, 2 (2019), 1811.08843.
  - [26] A. Geralico, F. Pompei, and R. Ruffini, *International Journal of Modern Physics: Conference Series* **12**, 146 (2012).